Amino Acids (2010) 39:1521–1536
DOI 10.1007/s00726-010-0621-4

ORIGINAL ARTICLE

Acute cholesterol depletion leads to net loss of the organic osmolyte taurine in Ehrlich Lettré tumor cells

Kasper Rømer Villumsen · Lars Duelund · Ian Henry Lambert

Received: 30 December 2009 / Accepted: 5 May 2010 / Published online: 25 May 2010

Abstract In mammalian cells, the organic osmolyte taurine is accumulated by the Na-dependent taurine transporter TauT and released though the volume- and DIDS-sensitive organic anion channel. Incubating Ehrlich Lettré tumor cells with methyl-β-cyclodextrin (5 mM, 1 h) reduces the total cholesterol pool to 60 ± 5% of the control value. Electron spin resonance data indicate a concomitant disruption of cholesterol-rich micro-domains. Active taurine uptake, cellular taurine content, and cell volume are reduced by 50, 20 and 20% compared to control values, respectively, whereas the passive taurine release is increased 4.5-fold under isotonic conditions following cholesterol depletion. However, taurine release under isotonic conditions is insensitive to DIDS and inhibitors of the volume-regulated anion channel. Uptake and release of meAIB are similarly affected following cholesterol depletion. Kinetic analysis reveals that cholesterol depletion increases TauT's affinity toward taurine but reduces its maximal transport capacity. Cholesterol depletion has no impact on TauT regulation by protein kinases A and C. Phospholipase A_2 activity, which is required for the activation of volume-sensitive organic anion channel (VSOAC), is increased under isotonic and hypotonic conditions following cholesterol depletion, whereas taurine release under hypotonic conditions is reduced following cholesterol depletion. Hence, acute cholesterol depletion of Ehrlich Lettré cells leads to reduced TauT and VSOAC activities and at the same time increases the release of organic osmolytes via a leak pathway different from the volume-sensitive pathways for amino acids and anions.

Keywords Phospholipase A_2 activity · Lysophospholipids · Cyclodextrin · TauT · VSOAC · Cell volume regulation

Abbreviations

CRAC	Cholesterol recognition/interaction amino acid consensus
dbcAMP	Dibutyryl cyclic AMP
DIDS	4,4-Diisothiocyano-2,2-stilbene acid
DCPIB	4-[(2-Butyl-6,7-dichloro-2-cyclopentyl-2,3-dihydro-1-oxo-1H-inden-5-yl)oxy]butanoic acid
ESR	Electron spin resonance
MβCD	Methyl-β-cyclodextrin
meAIB	α-Methylamino-isobutyric acid
NMDG	*N*-Methyl-D-glucamine
PKA	Protein kinase A
PKC	Protein kinase C
PLA_2	Phospholipase A_2
PMA	Phorbol myristate acetate
ROS	Reactive oxygen species
RVD	Regulatory volume decrease
VRAC	Volume-regulated anion channel
VSOAC	Volume-sensitive organic anion channel
TauT	Na^+-dependent taurine transporter

K. R. Villumsen · I. H. Lambert (✉)
Section for Cell and Developmental Biology,
Department of Biology, University of Copenhagen,
The August Krogh Building, Universitetsparken 13,
2100 Copenhagen Ø, Denmark
e-mail: ihlambert@bio.ku.dk

L. Duelund
Department of Physics and Chemistry, MEMPHYS,
University of Southern Denmark, Campusvej 55,
5230 Odense M, Denmark

Introduction

The interaction between cholesterol and other cell membrane components has been studied extensively in living cells and unilamellar vesicles made from lipids (Niu and Litman 2002; Pucadyil and Chattopadhyay 2006) and it has turned out that cholesterol in the plasma membrane is sequestered into rafts, i.e., highly ordered micro-domains, and that localization of proteins to these domains is facilitated by specific protein domains, e.g., CRAC (cholesterol recognition/interaction amino acid consensus) and sterol-sensing motifs (Epand 1778). Modulation of the cellular cholesterol content affects not only membrane dynamics but also the function of various proteins embedded in the plasma membrane, e.g., receptors (Burger et al. 2000; Gimpl et al. 2000), transporters for organic osmolytes (Cheema and Fisher 2008; Liu et al. 2009), gap junctions (Bastiaanse et al. 1997), Ca^{2+} channels (Bastiaanse et al. 1997), as well as the volume-regulated anion channel (VRAC; Klausen et al. 2006; Levitan et al. 2000).

Taurine homeostasis: cell function

Cell volume homeostasis is critical to cellular function, and the cellular strategies utilized to maintain and regulate cell volume under physiological and pathophysiological conditions have recently been reviewed (Hoffmann et al. 2009; Lambert 2004; Lambert et al. 2008). The cellular concentration of the organic osmolyte taurine (β-amino ethanesulfonic acid) is high in various types of mammalian cells (Bakker and Berg 2002; Blomstrand and Saltin 1999; Hoffmann and Lambert 1983; Holopainen et al. 1986; Kramer et al. 1981), and taurine has, besides its contribution to the intracellular pool of osmolytes and hence cell volume, been reported to exhibit anti-oxidative, anti-inflammatory and anti-apoptotic effects (Lambert 2004; Lambert et al. 2008; Lang et al. 2003; Schuller-Levis and Park 2003). The cellular taurine content is a balance between (a) endogenous synthesis from cysteine/methionine, (b) active uptake through the taurine-specific transporter TauT, and (c) passive release through a volume-sensitive transporter for organic osmolytes (see Huxtable 1992; Lambert 2004). TauT-mediated taurine uptake is driven by the electrochemical Na^+ gradient and kinetic analysis indicates that 2–3 Na^+ ions are required for initiation and effectuation of the translocation of one taurine molecule across the plasma membrane (Lambert 2004). TauT that belongs to the SLC6A family has been cloned (Uchida et al. 1992) and several TauT isoforms seem to be expressed in, e.g., Ehrlich ascites tumor cells (Poulsen et al. 2002) and NIH3T3 mouse fibroblasts (Voss et al. 2004). Taurine uptake via TauT in Ehrlich ascites tumor cells is subject to regulation by phosphorylation of the transporter or a putative regulator of the transporter, i.e., stimulation of protein kinase A (PKA) results in an increased taurine uptake, whereas stimulation of protein kinase C (PKC) results in a decreased taurine uptake and at the same time renders the taurine uptake process insensible toward PKA regulation (Mollerup and Lambert 1996). Inhibition of the constitutively active casein kinase 2 (CK2), on the other hand, reduces the Na^+:taurine stoichiometry and increases the maximal taurine uptake via TauT in NIH3T3 mouse fibroblasts (Jacobsen et al. 2008). Inhibition of protein phosphatases in Ehrlich ascites cells decreases taurine influx to a level similar to that of cells with activated PKC (Mollerup and Lambert 1998).

Taurine release under isotonic conditions is low but increases within minutes following hypotonic exposure. Various transport mechanisms have been proposed to mediate taurine release, i.e., TauT (working in reverse) seems to contribute to taurine release under isotonic conditions (Lambert and Hoffmann 1993) and during ischemia (Saransaari and Oja 1998), whereas a volume-sensitive organic anion channel, designated VSOAC and permeable to various organic osmolytes, mediates taurine release under hypotonic conditions (Hall et al. 1996; Lambert 2004). The molecular identity of VSOAC is yet unknown and although several anion efflux pathways have all been suggested to mediate taurine efflux under hypotonic conditions, i.e., the ubiquitously expressed, VRAC, ICln, ClC-3, phospholemman and the band 3 anion exchanger (AE1 isoform) none of them have unambiguously been demonstrated to fulfill the task. On the other hand, pharmacological profiling and analysis of the time courses for activation and inactivation of the taurine and anion efflux following hypotonic exposure indicate that the swelling-induced efflux pathways for the organic osmolytes and for anions in some cell systems could be separate entities (Diaz et al. 1993; Lambert 1998; Lambert and Hoffmann 1994; Moran et al. 1997; Pasantes-Morales et al. 1998; Stutzin et al. 1999). Diversity within volume-sensitive transporters for organic osmolytes has furthermore been demonstrated for brain cells (Franco et al. 2001; Mongin et al. 1999) and for polarized epithelial cells (Ullrich et al. 2006).

Activation of the taurine leak pathway in Ehrlich ascites tumor cells and NIH3T3 fibroblasts involves a phospholipase A_2 (PLA_2)-mediated release of arachidonic acid from the nuclear membrane (Pedersen et al. 2000, 2006) and oxidation of the fatty acid via the 5-lipoxygenase system (Lambert 2004). In several cell types, osmotic cell swelling is accompanied by an increased NADPH oxidase activity and hence an increased production of reactive oxygen species (ROS; Friis et al. 2008; Lambert 2003a, 2005; Ørtenblad et al. 2003; Varela et al. 2004), and in the case of the NIH3T3 fibroblasts, it has been demonstrated that

activation of the volume-sensitive NADPH oxidase system, a NOX4-isoform/p22phox complex, occurs at a step downstream to the activation of the PLA_2 (Friis et al. 2008; Lambert 2004). The volume-sensitive taurine efflux pathway is not activated by an increase in ROS per se but once the efflux pathway has been activated by osmotic cell swelling its activity becomes significantly potentiated by ROS (Lambert 2007). Similarly, it was recently demonstrated that exogenous H_2O_2 potentiates the swelling-induced Cl^- and K^+ currents in Ehrlich Lettré tumor cells (Lambert et al. 2009).

Exposure to cyclodextrins reduces total cholesterol levels in mammalian cells (Klausen et al. 2006; Yancey et al. 1996; Zidovetzki and Levitan 2007), and using fluorescent lipid probes it has been demonstrated that depletion of cellular cholesterol with methyl-β-cyclodextrin (MβCD) increases the lateral diffusion in, e.g., bovine hippocampal cell membranes (Pucadyil and Chattopadhyay 2006), demonstrating the role of cholesterol in membrane packing and fluidity. In the present work, we demonstrate that exposure of Ehrlich Lettré cells to MβCD under isotonic conditions leads to net loss of organic osmolytes and hence cell shrinkage due to a reduction in their accumulation and a concomitant increase in their release. Cholesterol depletion also stimulates PLA_2 activity, which is a prerequisite for the activation of the volume-sensitive efflux pathway for the organic osmolyte, but at the same time reduces the volume-sensitive release of taurine. Thus, acute reduction of the cellular cholesterol pool reduces the activity of active transporters and passive, volume-sensitive transporters for organic osmolytes in Ehrlich Lettré cells.

Materials and methods

Chemicals

Antibiotics (penicillin, streptomycin), fetal calf serum (Gibco) and trypsin (10×, Gibco) were from Invitrogen, Denmark. ^{3}H-labeled taurine and arachidonic acid were from GE Healthcare, UK. *N*-Methyl-D-glucamine (NMDG), RPMI-1640 (L-glutamine), MβCD, cholesterol, coprostanol, dibutyryl cyclic AMP (dbcAMP), phorbol myristate acetate (PMA), melittin, 4,4-diisothiocyano-2,2-stilbene acid (DIDS) and the spin probe methyl-5-doxyl-sterate were from Sigma Chemical Co., St. Louis, MO, USA. DCPIB was from Togris Bioscience, Bristol, UK. NS3728 was a kind gift from Palle Christophersen (Neurosearch, Ballerup, Denmark). The following stock solutions were prepared: MβCD (30 mM, serum-free medium), cholesterol (10 mM, ethanol), coprostanol (10 mM, ethanol), DIDS (20 mM, ethanol), dbcAMP (100 mM, NaCl medium), PMA (20 μM, ethanol), DCPIB (30 mM, ethanol), NS3728 (20 mM, DMSO) and melittin (1 mg ml$(H_2O)^{-1}$).

Inorganic media

Phosphate-buffered saline (PBS) contained 137 mM NaCl, 2.6 mM KCl, 6.5 mM Na_2HPO_4, and 1.5 mM KH_2PO_4. Isotonic standard NaCl medium contained 143 mM NaCl, 5 mM KCl, 1 mM Na_2HPO_4, 1 mM $CaCl_2$, 1 mM $MgSO_4$, and 10 mM *N*-2-hydroxyethyl piperazine-*N*′-2-ethanesulfonic acid. Hypotonic NaCl media were prepared by reduction of the NaCl content keeping the concentration of other ions and buffer constant. Isotonic NMDG medium was prepared by substitution of NMDGCl for NaCl. pH was adjusted to 7.4 in all media.

Cell cultures: cholesterol-depletion/-enrichment

Ehrlich Lettré ascites cells (ATCC, USA) were grown in Cellstar© T75 flasks (75 cm^2) or in six-well polyethylene dishes (9.6 cm^2 per well) as monolayer cultures in RPMI-1640 containing heat-inactivated fetal bovine serum (10%) and antibiotics (100 U ml(penicillin)$^{-1}$/0.1 mg ml(streptomycin)$^{-1}$). Cell lines were kept at 37°C/5% CO_2/100% humidity and passed on every 3–4 days using 0.5% trypsin in PBS to detach the cells. For cholesterol depletion, cells grown to 75–85% confluence (estimated by microscopy) were incubated for 1 h in serum-free RPMI-1640 medium and subsequently 1 h in RPMI-1640 medium containing 5 mM MβCD (37°C, 5% CO_2). Cyclodextrins bind proteins (Ohtani et al. 1989) and serum was omitted from the medium during the cholesterol depletion to avoid formation of MβCD protein complexes. Immediately before the experiment starts, the MβCD medium was removed and cells were washed in MβCD-free NaCl medium. For cholesterol enrichment, cholesterol was added to cells in NaCl medium at a final concentration of 10 μM.

Estimation of the cholesterol content

Total cellular cholesterol content, i.e., free cholesterol plus cholesterol esters, was estimated by an enzymatic colorimetric assay (CHOD-PAP, Roche Diagnostics, Manheim, Germany). Cells (80–90% confluence, control, cholesterol depleted, cholesterol enriched) were washed three times in 10 ml PBS. After removal of the final PBS wash, free cholesterol plus cholesterol esters were extracted by addition of 10 ml isopropanol (30 min). The isopropanol fraction from each flask was carefully transferred to separate glass containers for the estimation of cholesterol content. The remains of cells in each flasks were hydrolyzed overnight in 2 ml NaOH (1 M) and used for the

estimation of protein content (μg per flask) using the Lowry method (Lowry et al. 1951) and bovine serum albumin (BSA) as standard. The isopropanol was evaporated from the isopropanol fractions and the precipitate resuspended in 1 ml isopropanol. 10 μl sample was subsequently mixed with 1 ml R1 reagent from the "CHOD-PAP"-kit, left in the dark for at least 40 min and the absorbance was measured at 500 nm (Beckman-Coulter DU-800 spectrophotometer). Cholesterol standards in the range 0–8 μg ml^{-1} were used for the estimation of the total cholesterol content in the original flask (μg per flask). Cholesterol content was finally given relative to the protein content (μg $mg(protein)^{-1}$).

Estimation of taurine and meAIB influx

Taurine influx was estimated at room temperature as described for NIH3T3 fibroblasts (Voss et al. 2004). Briefly, Ehrlich Lettré cells were grown in six-well polyethylene dishes (80–90% confluence, 9.6 cm^2 per well) and washed three times by gentle aspiration/addition of 1 ml experimental solution. Following the final wash, cells in wells 1–5 were exposed to isotonic NaCl medium containing ^{3}H-taurine (2.4×10^4 Bq ml^{-1}, 24 nM taurine) for 3, 6, 9, 12 and 15 min, respectively. Cells in the sixth well were added to isotope-free NaCl medium and used for the estimation of the average protein content (mg protein per well) by the Lowry method and using BSA as standard (0–1.0 mg ml^{-1}). Taurine influx was terminated by aspiration of the extracellular medium followed by addition and aspiration of 1 ml ice-cold $MgCl_2$ (100 mM). Cells were lysed by addition of 200 μl 96% ethanol, the ethanol was evaporated and the cellular ^{3}H-taurine radioactivity was subsequently extracted by addition of 1 ml ddH_2O (1 h). Water extracts plus two additional washouts from wells 1 to 5 were transferred to a scintillation vial for the estimation of ^{3}H-labeled taurine radioactivity (β-scintillation counting, Ultima GoldTM). The total ^{3}H-taurine radioactivity taken up by the cells (cpm per well) was estimated as the sum of ^{3}H radioactivity in the cell extract plus the two water washouts. The cellular taurine content (cpm per mg protein), estimated from the ^{3}H-taurine content (cpm per well), and the protein content (mg protein per well) were plotted versus time (see Fig. 1b) and the taurine influx (nmol $g(protein)^{-1}$ min^{-1}) was estimated from the slope of the time plot, the extracellular specific activity (nmol cpm) and counting efficiency for ^{3}H. For the estimation of kinetic parameters and the effect of sterol replenishment, we used the ^{3}H-taurine content taken up by the cells within the initial 20 min (nmol $g(protein)^{-1}$). meAIB influx was estimated in a similar way using ^{14}C-meAIB (4.3 kBq ml^{-1}, 2 μM meAIB).

Estimation of the fractional rate constant for taurine and meAIB efflux

Efflux measurements were performed as described previously (Hall et al. 1996; Lambert 2003a). Ehrlich Lettré cells, grown to 80% confluence in six-well polyethylene dishes (9.6 cm^2 per well), were loaded for 2 h with 1 ml growth medium containing ^{3}H-taurine (74×10^3 Bq per well). The cells were washed with isotonic standard NaCl medium (three times) to remove excess extracellular ^{3}H-taurine and cellular debris. The efflux was initiated by aspiration of the medium followed by addition of one 600 μl experimental solution. After 2-min incubation, the entire medium was transferred to a scintillation vial and rapidly substituted by 600 μl fresh medium. This procedure was repeated every 2 min for 20 min. 1 ml NaOH was added to the well following removal of the extracellular medium at time 20 min to lyse the cells. The total pool of ^{3}H-labeled taurine in the cell system was estimated as the sum of ^{3}H-radioactivity in all the efflux samples, the NaOH lysate plus two final well washouts with ddH_2O (β-scintillation counting, Ultima Gold^{TM}). Release of taurine under the present experimental conditions follows a mono-exponential equation and the natural logarithm to the fraction of ^{3}H-labeled taurine remaining in the cells at a given time was plotted versus time (see Fig 6a). The fractional rate constant (k, min^{-1}) for the taurine efflux at a given time point was estimated as the negative slope of the graph between the time point and the proceeding time point (see, e.g., Fig. 6a). meAIB efflux was estimated and treated in a similar way using ^{14}C-meAIB.

Estimation of the fractional arachidonic acid release

Arachidonic acid release was estimated using a similar protocol as the one used for the estimation of taurine efflux with the exception that cells were loaded with ^{3}H-arachidonic acid (3 μCi per well, 24 h), 1% BSA was added to the efflux medium to trap released arachidonic acid. The release of ^{3}H-arachidonic at a given time point is shown as the total fraction released (%).

Estimation of the cellular amino acid content

The amino acid content was estimated by *ortho*-phthalaldehyde derivatization (OPA) followed by reversed phase high pressure liquid chromatography (Gilson: 322-Pump, 234-Autoinjector, 155-UV/VIS) as described for NIH3T3 mouse fibroblasts (see Voss et al. 2004). Briefly, Ehrlich Lettré cells, grown in T75 culture flask to 80% confluence, were lysed by addition of 1.8 ml of 4% sulfosalicylic acid. The lysate was scraped from the bottom with a rubber policeman, and homogenized by several passages through

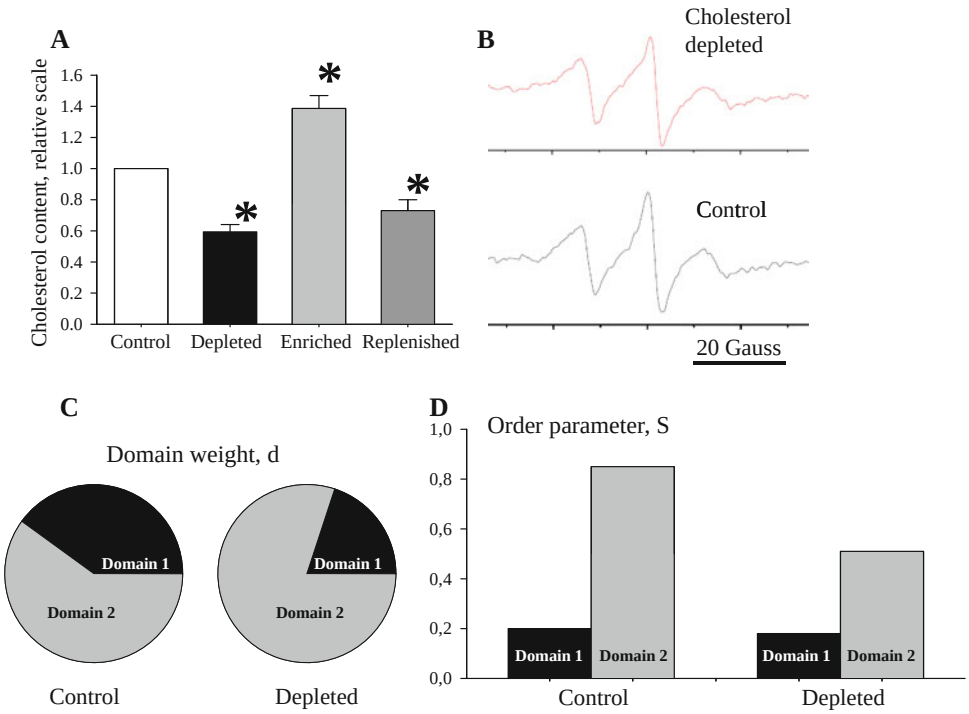

Fig. 1 The effect of cholesterol depletion on cholesterol content and membrane lipid domains in Ehrlich Lettré cells. **a** Cells, pre-incubated for 1 h in serum-free medium, were incubated for another hour in serum-free medium in the absence (control cells, *open bar*) or in the presence of either 5 mM MβCD (depleted cells, *black bar*) or 10 μM cholesterol (enriched cells, *light grey*). Cholesterol replenishment was obtained by 4 h exposure to 10 μM cholesterol following 1 h depletion (*dark grey bar*). Cholesterol content was estimated by the CHOD-PAP assay as indicated in "Materials and methods". The average cholesterol content is shown relative to the cholesterol content in control cells, estimated at 0.12 ± 0.02 μg cholesterol mg(protein)$^{-1}$ ($n = 4$). **b** ESR spectra from cholesterol-depleted cells and non-depleted control cells. All cells were incubated for 2 h in serum-free medium. Cholesterol-depleted cells were depleted with 5 mM MβCD (1 h). Cells were harvested by trypsination, pelleted by centrifugation, resuspended in serum-free medium and subsequently loaded with 5-methyl-doxyl-sterate as described in "Materials and methods". **c** The relative fractions of domains (*d*) found by simulation of the ESR spectra. **d** The order parameters for the individual domains found by the simulation of the ESR spectra. All simulation were performed with the EPRSIM program (Strancar et al. 2000)

a 1.2 mm diameter syringe. Aliquots were denaturated with NaOH and used for the estimation of the protein content by the Lowry procedure (BSA as protein standard). The residual homogenate was centrifuged (20,000*g*, 10 min), the supernatant was filtered (Milex-GV, 0.45 μm) and the amino acids were subsequently separated and quantified by OPA derivatisation followed by separation on a Nucleosil column (Macherey-Nagel, C18, 250/4, 5 μM) using gradient elution with acetonitrile/phosphate buffer (12.5 mM, pH 7.2) and UV absorption (330 nm). Amino acid standards (0.1 mM) were used for the quantitative estimation of the content of amino acids. The cellular amino acid content (μmol g(protein)$^{-1}$) was estimated from the amino acid and protein content.

Electron spin resonance (ESR) spectroscopy

Cells were grown in eight T75 culture flasks (80–90% confluence): four for non-depleted controls and four for cholesterol depletion. The cells were harvested by trypsination, and subsequently resuspended in 4 ml serum-supplemented growth medium. The cells from each experimental setup were pooled into centrifuge tubes, and pelleted by centrifugation, at 1,500 rpm for 3 min. After centrifugation, the supernatant was carefully removed by aspiration and the pellets were resuspended in 2 ml growth medium. 1 ml of this cell suspension from each tube was then transferred to glass tubes coated with a thin film of spin labels (60 μl 0.1 mM methyl-5-doxyl-sterate dissolved in ethanol, solvent evaporated on a rotary evaporator). Each glass tube was shaken for 10 min at 4°C, and then pelleted once again at 1,500 rpm for 3 min. The majority of the supernatant was aspirated, and the pelleted cells were resuspended in the remaining supernatant. 50 μl cell suspension was transferred to hematocrit-glass tubes, which was placed in a standard 4 mm OD ESR tube and placed in the ESR spectrometer (Bruker EMX Plus, Bruker Biospin Rheinstetten, Germany). The sample temperature was set to 37°C with the internal temperature controller. All spectra obtained were X-band spectra (Microwave

frequency ≈9.43 GHz) recorded with a power of 20 mW, a modulation frequency of 100 kHz, a modulation amplitude of 1 G and a time constant of 20.48 ms. Spectra were simulated with the program EPRSIM, version 4.99-2005 (Strancar et al. 2000).

Cell volume measurements

Control cells or cells depleted for cholesterol in serum-free medium (T175 flasks) were brought into solution by trypsination. Trypsin was inactivated by addition of serum containing RPMI-1640 after which the cell suspension was centrifuged for 45 s at 600*g*. Cells were resuspended in 3 ml standard NaCl medium and incubated for 10 min at 37°C. Absolute cell volumes were estimated after 20-fold dilution in standard medium (final cell density ≈ 90,000 cells ml^{-1}) by electronic cell sizing in a Beckmann Multisizer III, using the median of the cell volume distribution curves and latex beads (diameter 15 μm) for calibration.

Statistical analysis

Data are presented either as individual experiments that are representative of at least three independent sets of experiments or as mean values ± standard error of the mean (SEM). Statistical significance was estimated by Student's *t* test (one-tailed). For all statistical evaluations, *p* values <0.05 were taken to indicate a significant difference.

Results

Cholesterol depletion and its effect on physical properties of the cell membranes

The MβCD is a barrel-shaped water soluble structure with a hydrophobic interior which can accommodate hydrophobic molecules (Davis and Brewster 2004). In congruence with previous findings (Klausen et al. 2006), it is seen from Fig. 1a that the total cholesterol content in Ehrlich Lettré cells is reduced by 40% following 1-h incubation with 5 mM MβCD but increased by 40% following supplementation with 10 μM cholesterol for 1 h. However, reintroducing 10 μM cholesterol for 4 h to cells depleted for 1 h fails to produce a significant increase in the cholesterol content. Using electron density (Mathai et al. 2008) and ESR measurements (Swamy et al. 2006), it has previously been demonstrated that cholesterol affects the packing of components within each leaflet of the plasma membrane. To investigate whether cholesterol depletion affected the physical properties of the Ehrlich Lettré cell membranes, we used ESR in combination with computer simulation (EPRSIM program, Strancar et al. 2000). The most important parameters in the simulations are the order parameter (*S*), the fluidity in the form of the rotational correlation time (τ), and the numbers of different populations of the spin label and the weight of these. The order parameter gives information about the degree of order in the membrane and ranges from 0 in an isotropic environment to 1 for a perfect crystalline environment. The fluidity is the inverse of the viscosity and is in the simulations given as the rotational correlation time, which is linked to the diffusion constant (*D*), i.e., $\tau = 1/6D$. In a membrane system, the order parameter is mainly determined from how *large* movements the spin label is capable of, whereas the correlation time is primarily determined from how *fast* these movements are. It should be noted that they manifest themselves in different ways in the ESR spectra, which makes it possible to reliable separate these effects. The order of the membrane primarily modifies the splitting of the spectrum, i.e., the distance between the outer parts of the signal, whereas the correlation time modulates the width and the shape of the lines. Figure 1b shows the ESR spectra of the methyl-5-doxylsterate, recorded from cholesterol-depleted (top trace) and non-depleted control (lower trace) Ehrlich Lettré cells. In both cases, the best fit was obtained using two populations with parameters typical for membranes and we therefore distinguish between these two membrane types, termed domain 1 and domain 2. The domain weight, i.e., the relative amount of each domain, is given in Fig. 1c and the order parameters found for the two domains are shown in Fig. 1d. Based on the high-order parameter, domain 2 is taken to represent cholesterol-rich domains. Upon cholesterol depletion, the order parameter for domain 2 is decreased and the relative weight of domain 2 is increased. This indicates that cholesterol depletion in the Ehrlich Lettré cells disrupts cholesterol-rich domains and the remaining cholesterol becomes scattered into the bulk membrane.

Cholesterol depletion and its effect on taurine and meAIB uptake

To test whether cholesterol depletion affects the taurine homeostasis in Ehrlich Lettré cells, we estimated the cellular taurine content in non-depleted control cells and in cholesterol-depleted cells. In five sets of experiments, the cellular content of glycine, taurine and the taurine precursor hypotaurine in unpertubated cells was estimated at 113 ± 23, 69 ± 9 and 40 ± 4 μmol $g(protein)^{-1}$, respectively. Using average values for cell volume (3.24 ml(cell water) $g(cell\ dry\ weight)^{-1}$; Hoffmann et al. 1986) and protein content (0.78 g(protein) $g(cell\ dry\ weight)^{-1}$; Hoffmann and Lambert 1983), the amino acid content values equal cellular

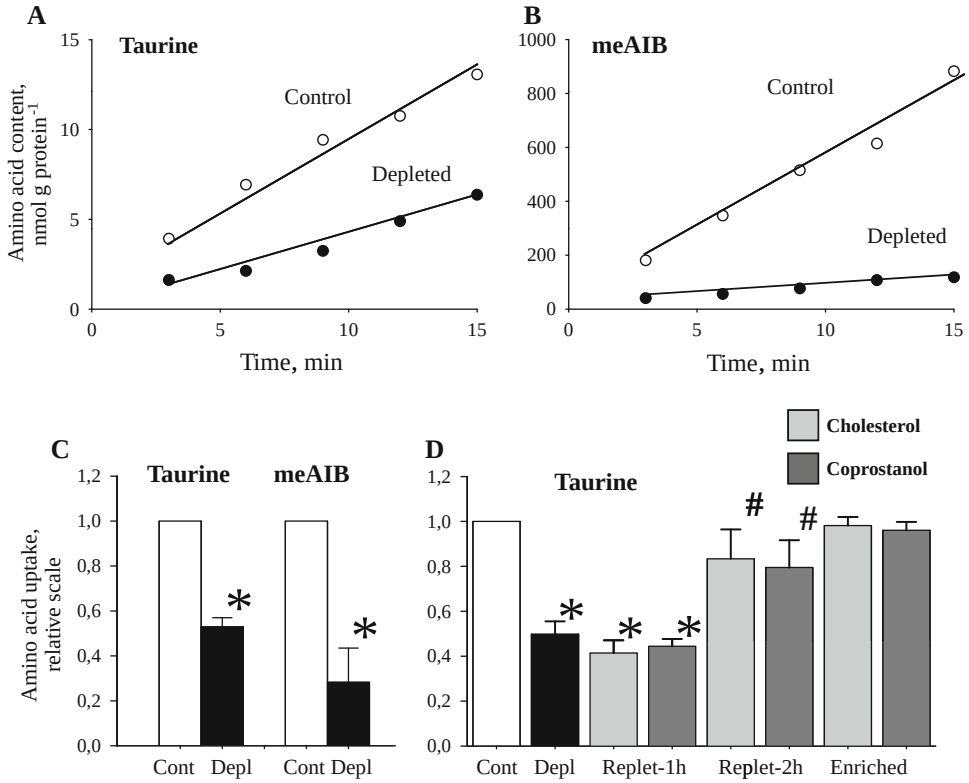

Fig. 2 Taurine and meAIB uptake in Ehrlich Lettré cells following modulation of the sterol content. The initial ^{3}H-taurine and ^{14}C-meAIB uptake was followed with time in Ehrlich Lettré cells under serum-free conditions in control cells, cholesterol-depleted cells (5 mM MβCD, 1 h), sterol-enriched cells (10 μM cholesterol/coprostanol, 1 h) or sterol-repleted cells (5 mM MβCD for 1 h followed by 10 μM cholesterol/coprostanol for 1 or 2 h). **a**, **b** ^{3}H-taurine and ^{14}C-meAIB uptake (cpm mg(protein^{-1})) plotted against time (min) in control cells (*open symbols*) and cholesterol-depleted cells (*closed symbols*). *Curves* are representative of 26 (taurine) and 3 (meAIB) sets of experiments. **c** Initial taurine and meAIB influx in control cells (*open bars*) and cholesterol-depleted cells (*black bars*). Influx (nmol g(protein^{-1}) min^{-1}) was estimated from the slope (cpm mg(protein)$^{-1}$ min^{-1}) of curves similar to those shown in **a/b** and the extracellular specific activity (cpm nmol^{-1}). Values are given relative to control values, i.e., 1.06 ± 0.08 nmol g(protein)$^{-1}$ min^{-1} (taurine, $n = 26$) and 64 ± 46 nmol g(protein)$^{-1}$ min^{-1} (meAIB, $n = 3$). **d** Taurine influx in control cells (*open bar*), cholesterol-depleted cells (*black bar*), cholesterol-enriched/cholesterol-repleted (1 h/2 h) (*light grey bars*), or coprostanol-enriched/coprostanol-repleted (1 h/2 h) (*dark grey bars*). Taurine influx is given relative to the influx in control cells and represents the mean values from four sets of paired experiment. *Significantly reduced compared to control values. #Significantly increased from values in cholesterol-depleted cells

concentrations of 28 ± 6 mM glycine, 17 ± 2 mM taurine and 10 ± 1 mM hypotaurine. Cholesterol depletion (5 mM MβCD, 1 h) was in five sets of experiments found to reduce the cellular glycine, taurine and hypotaurine content to 82 ± 9, 80 ± 9 and 71 ± 1% of the original content, respectively. Furthermore, estimation of the absolute cell volume on trypsinized Ehrlich Lettré cells indicated that the cholesterol depletion reduced the cell volume significantly by 20%, i.e., from 1,967 ± 56 to 1,576 ± 83 μm^3 (3 sets of paired experiments). It is noted that cholesterol depletion partly activates the VRAC under isotonic conditions (Klausen et al. 2006), and as the Ehrlich ascites cells are permeable to potassium under isotonic condition (Lambert et al. 1989), it is most likely that the reduction in cell volume following acute cholesterol depletion reflects net loss of organic osmolytes as well as KCl.

The data in Figs. 2 and 3 were performed in order to test whether the reduction in the taurine content following cholesterol depletion reflected a reduced uptake of amino acids. From Fig. 2a, it is seen that taurine uptake is reduced in Ehrlich Lettré cells depleted for 1 h with 5 mM MβCD. Estimation of the initial taurine influx indicated that the cholesterol depletion reduced the taurine influx significantly to approximately 50% of the influx in non-depleted control cells (Fig. 2c). From Fig. 2b and c, it is seen that the influx of meAIB, a synthetic amino acid which is a highly selective substrate for the low affinity, alanine-preferring amino acid transporter, is also significantly reduced in cholesterol-depleted cells when compared to control cells. Hence, cholesterol depletion seems to reduce the accumulation of organic osmolytes in Ehrlich Lettrè cells via TauT as well as transporters for neutral amino acids.

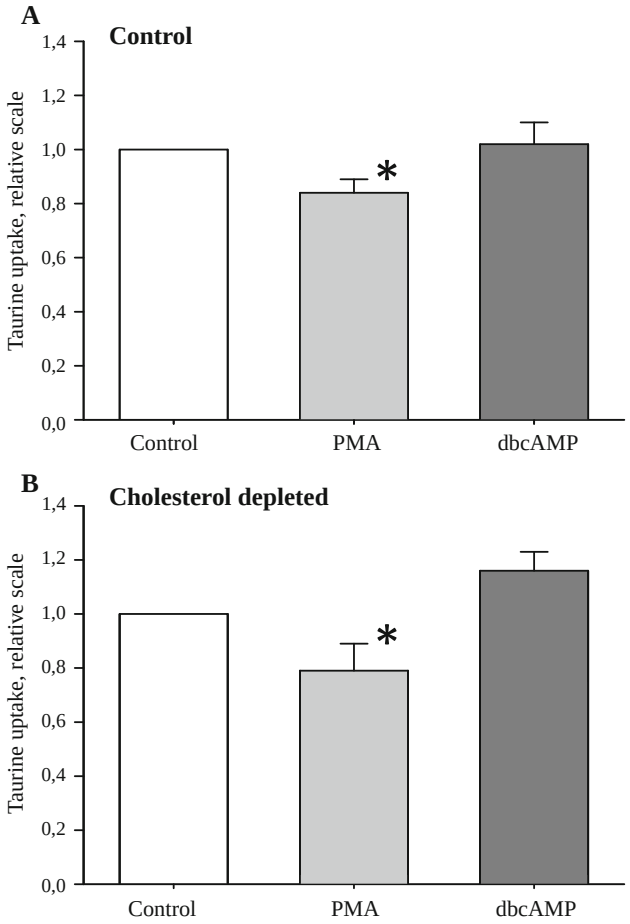

Fig. 3 The effect of PKA and PKC on taurine uptake in control and cholesterol-depleted Ehrlich Lettré cells. Taurine uptake was estimated in non-depleted control cells and cholesterol-depleted cells as indicated in Fig. 2. **a**, **b** PMA (10 nM, PKC activation) and dbcAMP (0.5 mM, PKA activation) were present from 10 min before and during the influx experiment. Values for taurine uptake are given relative to values for non-depleted control cells (**a**) or cholesterol-depleted control cells (**b**) and represent 11 (dbcAMP) and 7 (PMA) sets of paired data. *Significantly different from the respective control values

Acute cholesterol supplementation (10 μM, 1 h) had no significant effect on the taurine uptake (Fig. 2d). However, the effect of cholesterol depletion on the taurine uptake is reversed following reintroduction of cholesterol. This is seen from Fig. 2d, where normal taurine transport activity is restored following 2 h cholesterol replenishment. The effect of cholesterol replenishment on the taurine uptake is mimicked by coprostanol (5β-cholestan-3β-ol) (Fig. 2d). Coprostanol is formed by biohydrogenation of cholesterol (cholestan-3β-ol) and is considered to be a membrane inactive sterol (Stottrup and Keller 2006; Xu and London 2000). Thus, the configuration of the sterol rings' structure seems to be of minor importance for restoration of the taurine transporter TauT's activity.

Cholesterol depletion is previously reported to activate PKC (Kabouridis et al. 2000) and as PKC activation and PKC-mediated phosphorylation of the taurine transporter TauT (Ser^{322}) are known to reduce the taurine influx in several cell types (Han et al. 1999; Lambert 2004), we tested the effect of PKC activation on the initial taurine influx in cholesterol-depleted cells as well as non-depleted control cells. From Fig. 3, it is seen that exposure to PMA reduces the initial taurine influx to the same degree under normal control and cholesterol-depleted condition, i.e., there is no apparent synergistic effect of cholesterol depletion and PKC stimulation. Stimulation of PKA with exogenous addition of 0.5 mM dbcAMP, which is previously shown to stimulate taurine influx in the non-adherent Ehrlich ascites tumor cells (Mollerup and Lambert 1996), has no significant effect on taurine influx in control or cholesterol-depleted Ehrlich Lettré cells. Thus, the reduction in taurine uptake following cholesterol depletion does not seem to reflect modulation of the interaction between the taurine uptake system and PKC/PKA.

To test whether the reduced taurine influx in cholesterol-depleted cells could be explained by altered transport kinetics for TauT, we estimated the taurine influx as a function of the extracellular taurine concentration (Fig. 4a, b) and the extracellular Na^+ concentration (Fig. 4c, d). Fitting the data to a Michaelis–Menten equation (taurine saturation experiments) and a Hill type equation (Na^+-dependent taurine uptake), it was found that cholesterol depletion reduced the maximal taurine uptake (V_{max}) by approximately 50% (Fig. 4b, d) as well as the extracellular taurine concentration required for half maximal taurine uptake (K_m) (Fig. 4b). The affinity of TauT toward Na^+ and the Na^+:taurine transport stoichiometry were not affected by cholesterol depletion (Fig. 4d). The uptake by the non-saturable component (k value), which has previously been suggested to represent a second, Na^+-dependent system with low taurine affinity (Lambert 1984), was similarly reduced to 55 ± 20% by cholesterol depletion ($p = 0.07$). It is noted that cholesterol depletion increases the taurine leak under isotonic conditions (see below), which would increase the extracellular taurine concentration during the influx estimation and hence (a) shift the taurine saturation curve to the right and (b) reduce the extracellular specific activity for labeled taurine, causing an under-estimation of the influx (Fig. 4a, cholesterol-depleted cells). However, the extracellular specific activity for the artificial substrate meAIB is not affected by leak from the cells. Thus, even though the increase in the affinity of TauT toward taurine (K_m) and the reduction in the transport capacity (V_{max}) following cholesterol depletion might be overestimated, they are still taken to indicate that cholesterol depletion affects the taurine-TauT kinetics.

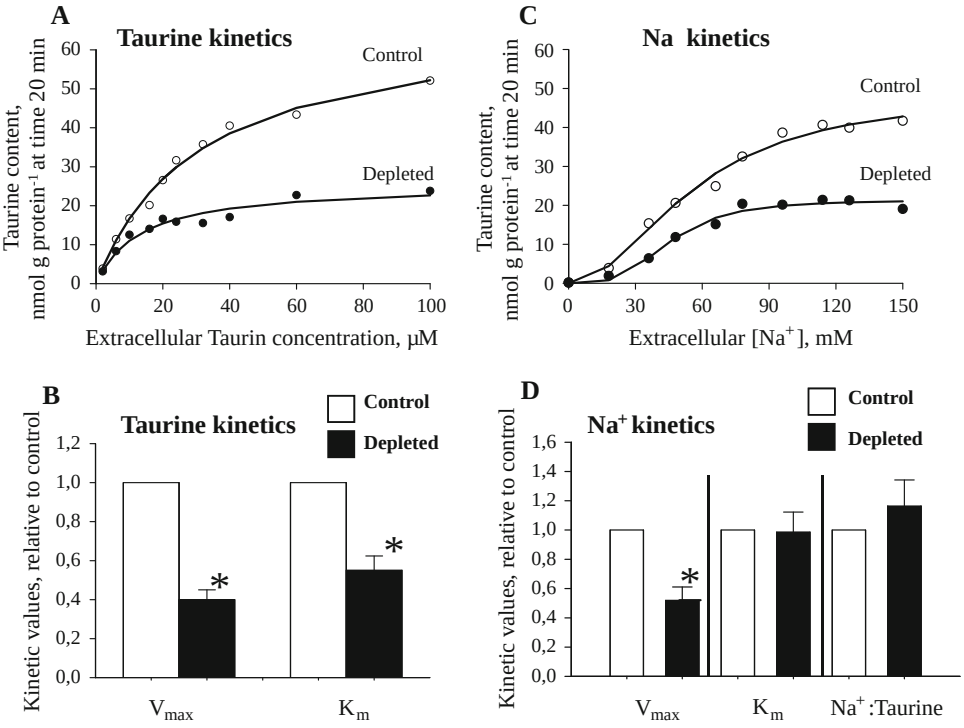

Fig. 4 The effect of cholesterol depletion on kinetic transport parameters for taurine uptake via TauT in Ehrlich Lettré cells. Control cells were incubated for 2 h in serum-free medium. Cholesterol-depleted cells were incubated for 1 h in serum-free medium followed by 1 h in serum-free medium containing 5 mM MβCD. Taurine uptake (nmol g(protein)$^{-1}$ at time 20 min) was estimated from the ^{3}H-radioactivity (cpm) accumulated within the 20 min and the extracellular specific activity (cpm nmol^{-1}). **a** Taurine saturation kinetics. Following the pre-incubation period, cells were washed in isotonic NaCl medium containing taurine in the concentration range from 2 to 100 µM and subsequently exposed for 20 min to a similar taurine concentration plus ^{3}H-labeled taurine. Taurine uptake in non-depleted control and cholesterol-depleted cells was plotted against the extracellular taurine concentration (µM, [Taurine]). The *curves* are representative of six sets of paired experiments. *Solid lines* represent data fitted (SigmaPlot 10.0) to a Michaelis–Menten equation: influx = $(V_{max}[\text{Taurine}])/(K_m + [\text{Taurine}]) + k[\text{Taurine}]$, where V_{max} is the maximal taurine uptake, K_m is the extracellular taurine concentration required for half maximal uptake, and k is a constant. **b** Kinetic values for taurine-dependent taurine uptake. V_{max}, K_m and k values in control cells were in six experiments estimated at 40.5 ± 7.4 nmol g(protein)$^{-1}$ 20 min^{-1}, 20 ± 3 µM taurine, and 0.23 ± 0.07 ml g(protein)$^{-1}$ 20 min^{-1}, respectively. V_{max} and K_m were estimated in cholesterol-depleted cells (*black bars*) and given relative to values from non-depleted control cells (*open bars*). Relative values are given as mean values ± SEM of the six independent sets of experiments. **c** Na^+ saturation kinetics. Following the pre-incubation period, cells were washed in isotonic Na^+/NMDG media, where the extracellular Na^+ concentration was varied between 0 and 150 mM, adjusting the osmolarity to isotonicity with NMDGCl and subsequently exposed to ^{3}H-labeled taurine for 20 min. Taurine uptake in non-depleted control and cholesterol-depleted cells was plotted versus the extracellular Na^+ concentration (mM, [Na^+]). The *curves* are representative of five sets of experiments. The *solid lines* indicate values fitted (SigmaPlot 10.0) to a Hill type equation: $Y = (V_{max}[Na^+]^n)/((K_{Na})^n + [Na^+]^n)$, where V_{max} is the maximal taurine uptake, K_{Na} is the Na^+ concentration required for half maximal taurine uptake and n is the number of Na^+ ions required for initiation of the uptake of one taurine. **d** Kinetic values for Na^+-dependent taurine uptake. V_{max}, K_{Na} and the Na:taurine stoichiometry in control cells were in five experiments estimated at 68 ± 19 nmol g(protein)$^{-1}$ 20 min^{-1}, 77 ± 10 mM Na^+, and 2.0 ± 0.1, respectively. Values in cholesterol-depleted cells (*black bars*) are given relative to data from non-depleted, control cells (*open bars*). Relative values are given as mean values ± SEM of the five independent sets of experiments. *Significantly reduced compared to non-depleted, control cells

Cholesterol depletion and its effect on taurine release under isotonic conditions

Release of taurine from Ehrlich Lettré cells follows a mono-exponential function. This is seen from Fig. 5a where the natural logarithm to the fraction of ^{3}H-labeled taurine remaining in preloaded cells is plotted versus time. Using rate constants, estimated from the slope of the release curves in control and cholesterol-depleted cells (Fig. 5a), it is estimated that taurine release under isotonic conditions is increased approximately 4.5-fold following cholesterol depletion (Fig. 5c). Release of meAIB is concomitantly increased by cholesterol depletion (Fig. 5b, c). It is noted that taurine efflux can be estimated as the product of the fractional rate constant (min^{-1}) and the cellular taurine pool (µmol g(protein)$^{-1}$), and taking the reduction in the cellular taurine content following the cholesterol depletion into consideration (see above), it is estimated that the cholesterol depletion more than triples the efflux of taurine under isotonic conditions. From

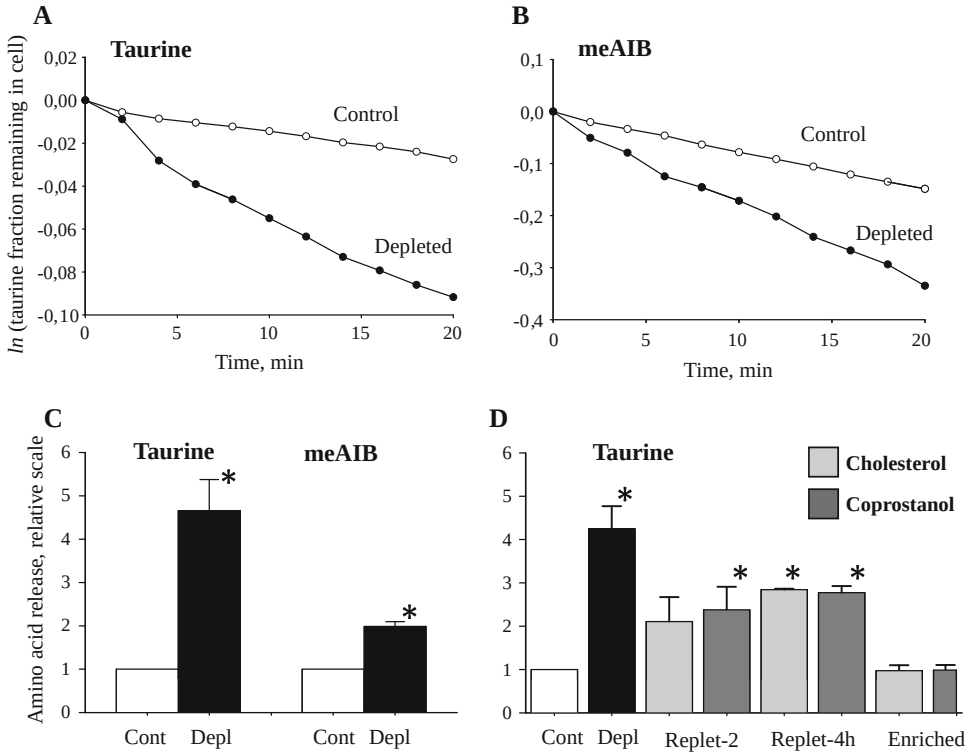

Fig. 5 Taurine and meAIB release under isotonic conditions in Ehrlich Lettré cells following modulation of the sterol content. Ehrlich Lettré cells were pre-incubated in serum-free medium for 2 h in the presence of ^{3}H-labeled taurine or ^{14}C-labeled meAIB. Cholesterol depletion and sterol enrichment were obtained be exposing the cells during the last 1 h before the efflux experiment to 5 mM MβCD or 10 μM cholesterol/coprostanol, respectively. Sterol repletion was performed on cells pre-exposed to MβCD (5 mM, 1 h), washed and exposed to 10 μM cholesterol or coprostanol for 2 or 4 h. Following pre-incubation, the cells were washed and the efflux experiment conducted in isotonic NaCl medium as indicated in "Materials and methods". **a** Taurine release under isotonic conditions in non-depleted control cells (*open symbols*) and cholesterol-depleted (*filled symbols*) cells. Release is shown as the change in the fraction of ^{3}H-labeled taurine remaining in the cell (*ln* scale) plotted versus time. **b** meAIB release under isotonic conditions in non-depleted control cells (*open symbols*) and cholesterol-depleted (*filled symbols*) cells. Release of meAIB was estimated and presented in the same way as for taurine. **c** The fractional rate constants (min^{-1}) for taurine and meAIB release in control and cholesterol-depleted cells. Rate constants under isotonic conditions were in each case estimated as the slope of the time traces (6–20 min) in **a** and **b**. Values for cholesterol-depleted cells (*black bars*) are given relative to the respective control values from non-depleted cells (*open bars*), i.e., 0.0013 ± 0.0001 min^{-1} (taurine, $n = 9$) and 0.0066 ± 0.0003 (meAIB, $n = 3$). **d** Taurine release following sterol repletion. Taurine release in control cells (*open bar*), cholesterol-depleted cells (*black bar*), cholesterol-enriched/cholesterol-repleted (2 h/4 h) (*light grey bars*), or coprostanol-enriched/coprostanol-repleted (2 h/4 h) (*dark grey bars*) are given relative to the release in control cells and represent the mean values from three sets of experiment. *Values are significantly increased compared to control cells

Fig. 5d, it is seen that acute sterol enrichment (cholesterol, coprostanol) has no significant effect on the taurine efflux under isotonic conditions. On the other hand, 4-h sterol replenishment partly reverses the effect of cholesterol depletion, i.e., the taurine release under isotonic conditions is still significantly increased compared to control cells.

Cholesterol depletion and its effect on PLA_2 activity

Stimulation of PLA_2 activity and hence mobilization of arachidonic acid is a prerequisite for the activation of the volume-sensitive taurine efflux pathway in Ehrlich Lettré cells (Lambert 2007). To test whether cholesterol depletion affected the PLA_2 activity, we estimated taurine release (Fig. 6) and arachidonic acid release (Fig. 7) in non-depleted and cholesterol-depleted Ehrlich Lettré cells following exposure to melittin under isotonic conditions. Melittin is a cationic, amphiphilic peptide that has no effect on the kinetic properties of PLA_2 per se but is instead reported to promote substrate replenishment by direct exchange of the product of the PLA_2-mediated hydrolysis (Cajal and Jain 1997). We have previously demonstrated that addition of melittin to NIH3T3 cells elicits arachidonic acid release (secretory PLA_2 and Ca^{2+}-independent $iPLA_2$ activity) as well as taurine release under isotonic conditions, and that the swelling-induced and the melittin-induced signaling pathway for taurine efflux share intracellular signaling elements as well as a common efflux

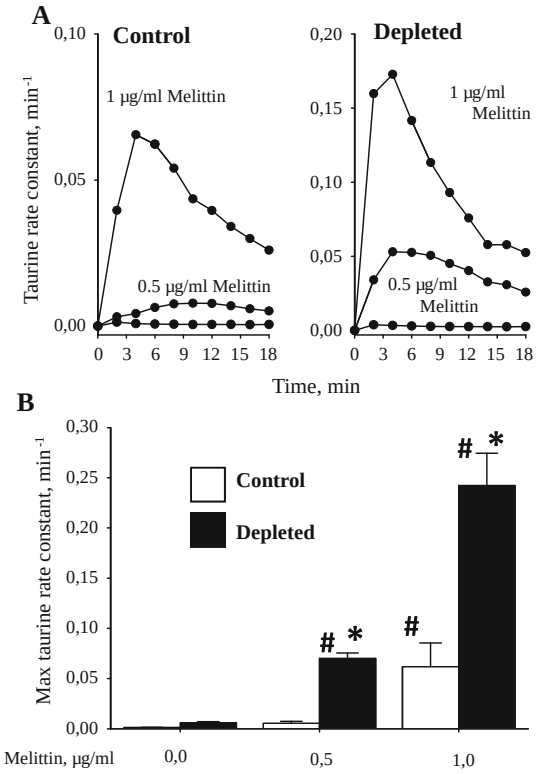

Fig. 6 The effect of cholesterol depletion on melittin-induced taurine release in Ehrlich Lettré cells. Cells were prepared and taurine release estimated as indicated in 5. ^{3}H-taurine release was followed with time under isotonic conditions in the absence or presence of melittin (0.5, 1.0 µg ml^{-1}). **a** Taurine release in non-depleted control (*left frame*) and cholesterol-depleted cells (*right frame*). Release is shown as the fractional rate constant for taurine release (min^{-1}) plotted versus time. Melittin when present was added at time zero. **b** Mean rate constants (min^{-1}) for taurine release under isotonic conditions (300 mOsm) and maximal rate constants (min^{-1}) obtained after melittin exposure. Values were obtained from curves similar to those presented in **a** from non-depleted control and cholesterol-depleted cells. All values are shown as mean values from three sets of experiments. *Significantly increased compared to non-depleted cells with the same concentration of melittin

pathway (Lambert 2003b). From Fig. 6a, it is seen that melittin induces a transient release of taurine from Ehrlich Lettré cells under isotonic conditions and that the effect is dose-dependent. Cholesterol depletion improves the effect of melittin (Fig. 6a, compare left and right frame). Using the maximal rate constant for taurine release obtained under isotonic conditions, it is estimated that the effect of 1.0 µg ml^{-1} melittin is a fourfold increase in the fractional rate constant for taurine release in cholesterol-depleted cells compared to the non-depleted control cells (Fig. 6b). From Fig. 7, it is seen that the release of arachidonic acid from Ehrlich Lettré cells to the extracellular compartment under isotonic conditions increases with time and that cholesterol depletion improves the arachidonic acid release in the absence (Fig. 7a) and the presence of melittin (0.5 µg ml^{-1}, Fig. 7b). Release of arachidonic acid is also increased under hypotonic conditions following cholesterol depletion (Fig. 7c). Thus, cholesterol depletion leads to an increase in PLA_2 activity and taurine release under isotonic conditions.

Cholesterol depletion and its effect on taurine release under hypotonic conditions

From Fig. 8, it is seen that taurine release in Ehrlich Lettré cells is increased under hypotonic conditions (Fig. 8a, left panel) and that the maximal rate constant for taurine release, obtained under hypotonic conditions, increases with decreasing tonicity (Fig. 8b, open bars). Taurine release is similarly increased under hypotonic conditions in cholesterol-depleted cells (Fig. 8a, right panel, b, grey bars). To test whether the increase in taurine release under isotonic conditions following cholesterol depletion reflected an increased activity of the volume-sensitive release pathway for organic osmolytes, we estimated the rate constant for taurine release in non-depleted control and cholesterol-depleted cells under isotonic conditions in the presence of 20 µM DIDS, i.e., at a concentration sufficient to suppress the volume-sensitive taurine efflux pathway (Lambert 2004). The relative rate constants under isotonic conditions for taurine release in DIDS-treated cells compared to cells with no DIDS were estimated at 1.0 ± 0.2 and 1.8 ± 0.5 ($n = 3$) in control and cholesterol-depleted cells, respectively. The use of DIDS to inhibit the volume-sensitive efflux pathway is problematic because of the non-specificity of this compound for other anion channels and transporters. However, the anion channel blockers DCPIB (Raucci Jr et al. 2010) and NS3728 (Poulsen et al. 2010) were also without any significant effect on the taurine release under isotonic conditions following cholesterol depletion, i.e., the relative rate constants for taurine release in DCPIB-treated cells (10 µM, $n = 4$) compared to cells with no DCPIB were 1.1 ± 0.2 and 1.6 ± 0.2 in control and cholesterol-depleted cells, respectively, whereas the equivalent values for (NS3728, 5 µM, $n = 3$) were 0.5 ± 0.1 and 2.7 ± 0.5. Thus, the increase in organic osmolyte release following acute cholesterol depletion under isotonic conditions does not seem to involve the VRAC or VSOAC. Plotting the maximal rate constant for the taurine release in cholesterol-depleted cells under hypotonic conditions relative to the rate constant for cholesterol-depleted cells under isotonic conditions indicates that cholesterol depletion reduces the swelling-induced taurine release significantly in the range 280–200 mOsm (Fig. 8b, black bars). Hence, cholesterol depletion seems to reduce TauT as well as VSOAC activities in Ehrlich Lettré cells.

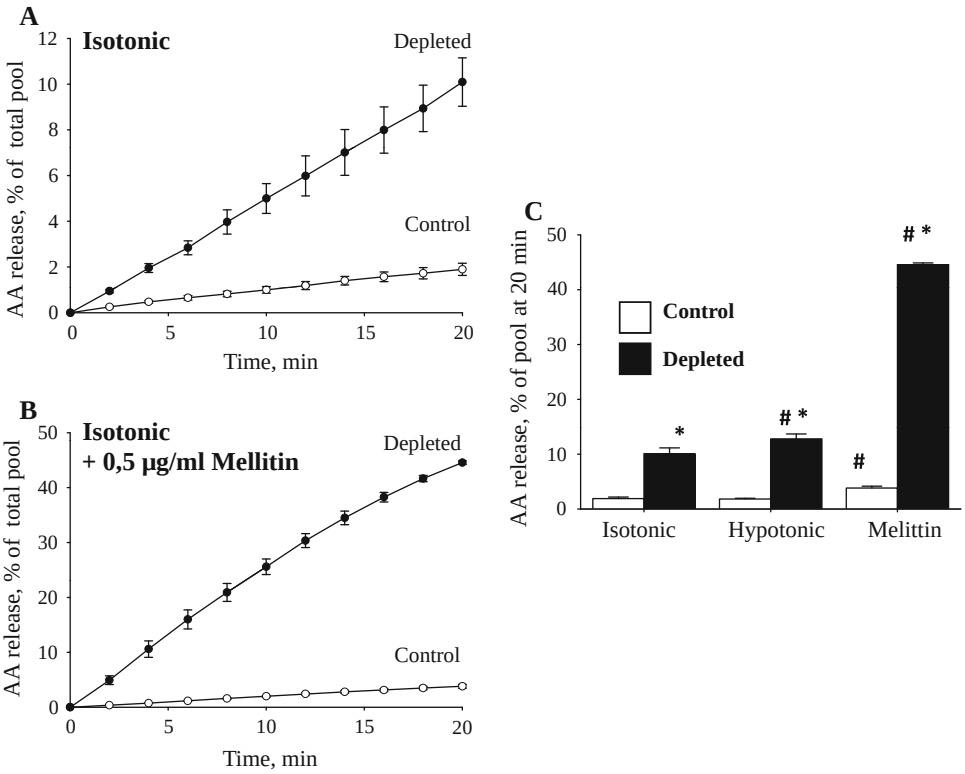

Fig. 7 The effect of cholesterol depletion on arachidonic acid release in Ehrlich Lettré cells. Cells were preloaded with ^{3}H-labeled arachidonic acid for 24 h and non-depleted control and cholesterol-depleted cells prepared as described in Fig. 5. Cells were washed three times in isotonic NaCl medium (300 mOsm) and the release of ^{3}H-arachidonic acid subsequently followed with time in isotonic NaCl medium or hypotonic NaCl medium (260 mOsm). 1% BSA was included in the media to trap ^{3}H-arachidonic. ^{3}H-arachidonic release in non-depleted, control cells (*open symbols*) and cholesterol-depleted cells (*closed symbols*) are expressed in fractions of the total pool (%). **a**, **b** Arachidonic acid release under isotonic conditions in the absence (**a**) or presence (**b**) of melittin (0.5 µg ml^{-1}). **c** Mean fractional ^{3}H-arachidonic release in control cells (*open bars*) and cholesterol-depleted cells (*black bars*) following 20 min exposure to isotonic NaCl medium, hypotonic NaCl medium or isotonic NaCl medium plus melittin (0.5 µg ml^{-1}). Data in **a**, **b** and **c** represent mean values from three sets of experiments. *Significantly increased by cholesterol-depletion. #Significantly increased by melittin treatment when compared to the relevant isotonic condition

Discussion

Changes in the cholesterol concentration have a major impacts on the physical properties of the membrane lipid bilayer, i.e., reduction in the cholesterol content increases the membrane fluidity, whereas an increase in the cholesterol content increases the bilayer thickness and drives the bilayer into a more rigid state (Xu and London 2000). Several transport processes and intracellular signaling events depend on intact cholesterol-rich micro-domains in the cell membrane, i.e., the VRACs in Ehrlich Lettré cells are sensitive to cholesterol depletion (Klausen et al. 2006), whereas protein tyrosine kinase activity and Ca^{2+} signaling in T cells have been associated with lipid rafts (Kabouridis et al. 2000).

Cholesterol depletion affects accumulation and release of organic osmolytes

In the present investigation, it is demonstrated that acute cholesterol depletion in Ehrlich Lettré cells under isotonic conditions results in a reduction in the active taurine uptake, an increase in the passive taurine release and consequently net loss of cellular taurine and reduction in cell volume. Accumulation of the synthetic amino acid meAIB from Ehrlich Lettré cells under isotonic conditions is similarly reduced and stimulated, respectively. meAIB is accumulated via the Na^{+}-dependent A-type transporter with a low substrate affinity. Hence, cholesterol depletion seems to reduce accumulation of amino acids and concomitantly favor their release. Protein kinases (PKC, PKA, CK2) have previously been shown to affect taurine uptake via TauT either through modulation of (a) maximal transport capacity, (b) affinities of TauT toward Na^{+} and taurine or (c) Na^{+}, taurine transport stoichiometry (Lambert 2004). However, shift in PKA/PKC activity and/or their accessibility to TauT do not seem to be involved in the reduction in taurine uptake following cholesterol depletion. On the other hand, kinetic analysis of taurine uptake indicated that cholesterol depletion is accompanied by a reduction in the maximal taurine

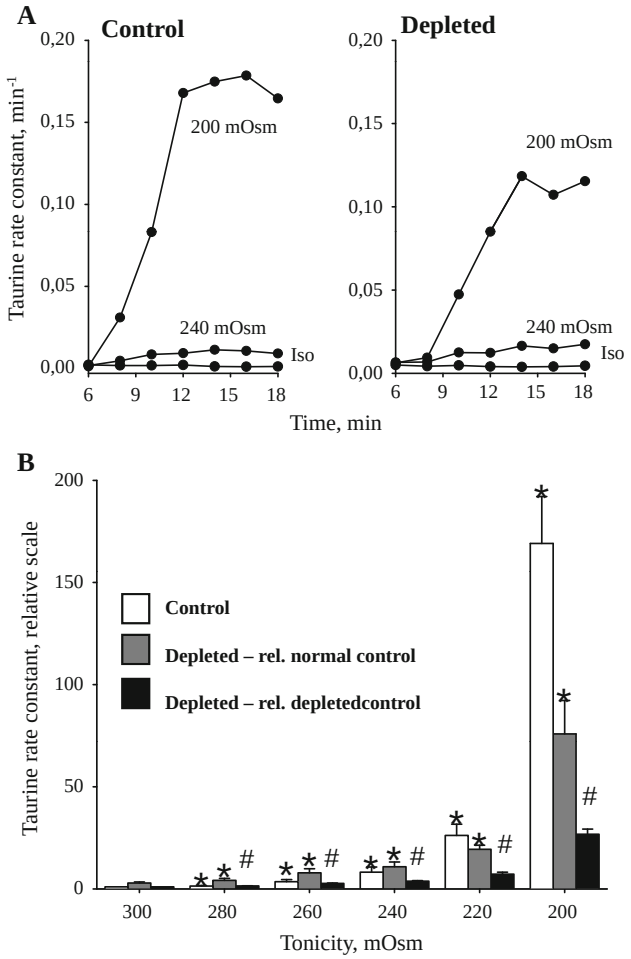

Fig. 8 The effect of cholesterol depletion on taurine release under hypotonic conditions in Ehrlich Lettré cells. Ehrlich Lettré cells were pre-incubated in serum-free medium for 2 h in the presence of ^{3}H-labeled taurine and cholesterol depleted as indicated in Fig. 5. Taurine release was followed with time in isotonic NaCl medium for 6 min and subsequently in hypotonic NaCl medium for another 12 min. The time course shown (6–18 min) represents release under hypotonic conditions. For time course under isotonic conditions, see Fig. 5. **a** Taurine release in non-depleted control cells (*left frame*) and cholesterol-depleted cells (*right frame*) under isotonic (Iso, 300 mOsm) and hypotonic (240 mOsm/200 mOsm). Release is shown as the fractional rate constant (min^{-1}) plotted versus time. **b** Mean rate constants for taurine release under isotonic conditions (300 mOsm) and maximal rate constants (min^{-1}) obtained under hypotonic conditions (280–200 mOsm). Values for the maximal rate constant obtained under hypotonic conditions in non-depleted cells are given relative to the isotonic value (*open bars*). Values for the maximal rate constant obtained under hypotonic conditions in cholesterol-depleted cells are given relative to the rate constant obtained under isotonic conditions for either non-depleted control cells (*grey bars*) or depleted cells (*black bars*). All values are shown as mean values from three sets of experiments. *Significantly increased compared to non-depleted isotonic control value. #Significantly increased compared to depleted isotonic control value

transport capacity of TauT and at the same time in an increased affinity of TauT toward taurine. This is in congruence with the effect of cholesterol depletion on glycine transporter GLYT1 in Chinese hamster ovary cells (Liu et al. 2009).

Opposing effects of cholesterol depletion on taurine release under isotonic and hypotonic conditions

PLA_2 activity has previously been demonstrated to be a prerequisite for the activation of the volume-sensitive taurine efflux pathway (Lambert 2004) and the increased PLA_2 activity and taurine release seen under isotonic conditions following cholesterol depletion could be taken to indicate that the set point for the volume-sensitive transporter for organic osmolytes had been shifted to a lower value. However, neither DIDS, which blocks the volume-sensitive organic osmolyte transporter at a low concentration, nor DCPIB and NS3728, which block the VRAC, reduced the taurine release under isotonic conditions in control or cholesterol-depleted cells. Hence, cholesterol depletion does not seem to shift the volume set point for the activation of VSOAC or facilitate taurine transport through VRAC. On the other hand, lysophospholipids which are PLA_2 products have been shown to stimulate taurine release, i.e., lysophosphatidic acid potentiates volume-sensitive taurine loss in NIH3T3 cells (Friis et al. 2008), whereas lysophosphatidylcholine induces taurine loss under isotonic conditions in various cell lines, e.g., HeLa cells (Lambert and Falktoft 2000; Lambert and Falktoft 2001), NIH3T3 mouse fibroblasts (Lambert and Falktoft 2001), C2C12 myotubes (Lambert et al. 2001), as well as ion current through mechano-gated cation channels (TREK-1, TRAAK) (Maingret et al. 2000). Hence, PLA_2-derived lysophospholipids could account for some of the effects on osmolyte transport seen in cholesterol-depleted cells.

VRAC in Ehrlich Lettré cells responds almost similarly to cholesterol depletion as VSOAC, i.e., mild hyposmotic exposure (300 mOsm → 255 mOsm), results in an increased anion current as well as max current relative to non-depleted control cells, whereas more severe hypotonic exposure (300 mOsm → 190 mOsm) results in identical current activation and max current in control and cholesterol-depleted cells (Klausen et al. 2006). However, comparing the rate constants for taurine release under hypotonic conditions to the rate constant for isotonic-depleted control cells reveals that cholesterol depletion actually reduces swelling-induced taurine release. PLA_2 is involved in the initiation of the signaling cascade in Ehrlich Lettré cells that leads to activation of the volume-sensitive taurine efflux pathway (Hoffmann et al. 2009; Lambert 2004; Lambert et al. 2008), and as PLA_2 activity is stimulated by cholesterol depletion, we suggest that the volume-sensitive leak pathway for organic osmolytes (VSOAC) just like Na^+-dependent transporters for amino acids (TauT, System A, GLYT1) is less active in cholesterol-depleted cells.

Cholesterol depletion, which is known to disrupt lipid micro-domains (Brown and London 2000; Zidovetzki and Levitan 2007) and to potentiate the anion conductance in various cell types (Klausen et al. 2006; Levitan et al. 2000; Romanenko et al. 2004), also potentiates the anion conductance in caveolin-deficient Caco-2 colonocytes as well as in sphingomyelase-treated Intestine 407 cell (Lim et al. 2006). This limits the role for disruption of cholesterol-rich domain on volume-sensitive ion transporters (VRAC) and most probably also the volume-sensitive transporter for organic osmolytes (VSOAC) following cholesterol depletion and points instead to a direct impact on the transporters due to modulation of the physical properties of the membrane bilayer. The intracellular signaling cascades and the volume-sensitive transporters for anions deviate in some cell lines from the signaling cascades and transporters for the organic osmolytes (Hoffmann et al. 2009) and as depletion of plasma membrane cholesterol increases membrane stiffness (Byfield et al. 2004), it is possible that the analogous response to cholesterol depletion seen with VRAC and VSOAC in Ehrlich Lettré cells partly reflects shift in direct cholesterol interaction with membrane imbedded, volume-sensitive transporters. Direct interaction between cholesterol and protein segments has been proposed to stabilize transmembrane domains of the acetylcholine receptor and to modulate the structural conversion of light activated rhodopsin (Burger et al. 2000).

Cholesterol depletion affects the domain distribution in the membrane lipid bilayer and the activity of the embedded transporter for taurine

The spin probe data (methyl-5-doxyl-sterate, ESR technique) indicate that acute cholesterol depletion (MβCD, 1 h) disrupts lateral membrane domains in Ehrlich Lettrè cells that are normally stabilized by high, local concentrations of cholesterol, i.e., the estimated order parameter for the large ordered domain (domain 2) in cholesterol-depleted cells is lower than the parameter for the ordered domain in control cells. This could indicate that cholesterol depletion disrupts membrane patches that are normally stabilized by cholesterol and that the remaining cholesterol becomes scattered into the bulk membrane. In agreement with previous publications (Klausen et al. 2006), we find that direct supplementation with exogenous cholesterol and acute cholesterol depletion with MβCD resulted in a significant increase and reduction in the total cholesterol content, respectively. However, the observation that TauT activity is partially regained after 2 h cholesterol replenishment whereas the volume-sensitive taurine release as well as the total cholesterol content is virtually unchanged could indicate that TauT and the volume-sensitive taurine transporter localize to separate sub-compartments of the cell membrane. The CHOD-PAP assay, used for estimation of the cellular cholesterol level, is sensitive to cholesterol as well as cholesterol esters, i.e., the change in the cholesterol pool reflects a shift in membrane bound cholesterol as well as in the pool of cholesterol esters. Using cyclodextrin-mediated depletion of radiolabeled cholesterol from CHO-K1 cells (Haynes et al. 2000), mouse L-cells, Fu5AH cells and human skin fibroblasts (Yancey et al. 1996), it has been demonstrated that cyclodextrin removes cholesterol from two separate pools, i.e., a fast pool (half-time 19–21 s) and a slow pool. The origin of the cholesterol pools has been discussed and it has been suggested that (a) they arise from cell membrane cholesterol (fast pool) and intracellular membranes (slow pool), or that (b) both pools are present in the cell membrane. In the latter case, kinetic differences could be due to transfer between intra- and extracellular leaflet (flip-flop) or that a fraction of the cholesterol is located to caveolae or rafts (Haynes et al. 2000; Lange and Steck 2008; Yancey et al. 1996; Zidovetzki and Levitan 2007). It is noted that sterol replenishment, i.e., reintroduction of cholesterol or coprostanol to MβCD-depleted Ehrlich Lettré cells, partly reverses the depletion-induced reduction in taurine uptake and taurine release under isotonic conditions, which is taken to indicate that sterols reestablish normal function of amino acid transporters under isotonic conditions. Incorporation of a protein in a lipid bilayer requires an increase in the bilayer surface area and as addition of cholesterol to a phospholipid bilayer increases the area expansion modulus and hence the energy to create a vacancy in the bilayer (McIntosh and Simon 2006), it is feasible that the reduction in TauT and VSOAC activity in cholesterol-depleted cells is caused by a reduction in the area expansion modulus and hence the number of active transporters in the membrane.

In conclusion, MβCD-mediated cholesterol depletion favors net loss of amino acids in Ehrlich Lettré cells under isotonic conditions, i.e., accumulation via Na^+-dependent transporters (TauT, System A, GLYT1) is reduced, and loss via a leak pathway different from the DIDS- and volume-sensitive leak pathway. The volume-sensitive transporter for organic osmolytes, on the other hand, is reduced following cholesterol depletion. The effect on the taurine uptake reflects a reduction in the maximal taurine uptake via TauT and an increase in the affinity of TauT toward taurine, whereas the increased taurine release under isotonic conditions reflects loss through a transporter different from VSOAC and VRAC. The volume leak pathway VSOAC is just like TauT less active following cholesterol depletion, most probably due to reduction in the area expansion modulus and hence the number of active transporters in the membrane. It is emphasized that cholesterol depletion leads to a significant reduction in the cell volume and that cell shrinkage is known to induce apoptosis in various cells (Hoffmann et al. 2009), i.e., the use of

cyclodextrins as drug carriers (Davis and Brewster 2004) might cause unintentional cell damage.

Acknowledgments The present work was supported by The Danish Council for Independent Research/Natural Sciences (Grant 272-07-0530, 272-08-0170, 21-04-0535), and The Danish Council for Independent Research/Medical Sciences (Grant 271-08-0520). The technical assistance of Dorthe Nielsen is gratefully acknowledged. Jacob Møller and Ronni Sander Frederiksen are acknowledged for contributing with experiments included in Figs. 2 and 4.

References

Bakker AJ, Berg HM (2002) Effect of taurine on sarcoplasmic reticulum function and force in skinned fast-twitch skeletal muscle fibres of the rat. J Physiol 538:185–194

Bastiaanse EM, Hold KM, Van der Laarse LA (1997) The effect of membrane cholesterol content on ion transport processes in plasma membranes. Cardiovasc Res 33:272–283

Blomstrand E, Saltin B (1999) Effect of muscle glycogen on glucose, lactate and amino acid metabolism during exercise and recovery in human subjects. J Physiol 514(Pt 1):293–302

Brown DA, London E (2000) Structure and function of sphingolipid- and cholesterol-rich membrane rafts. J Biol Chem 275:17221–17224

Burger K, Gimpl G, Fahrenholz F (2000) Regulation of receptor function by cholesterol. Cell Mol Life Sci 57:1577–1592

Byfield FJ, Aranda-Espinoza H, Romanenko VG, Rothblat GH, Levitan I (2004) Cholesterol depletion increases membrane stiffness of aortic endothelial cells. Biophys J 87:3336–3343

Cajal Y, Jain MK (1997) Synergism between melittin and phospholipase A(2) from bee venom: apparent activation by intervesicle exchange of phospholipids. Biochemistry 36:3882–3893

Cheema TA, Fisher SK (2008) Cholesterol regulates volume-sensitive osmolyte efflux from human SH-SY5Y neuroblastoma cells following receptor activation. J Pharmacol Exp Ther 324:648–657

Davis ME, Brewster ME (2004) Cyclodextrin-based pharmaceutics: past, present and future. Nat Rev Drug Discov 3:1023–1035

Diaz M, Valverde MA, Higgins CF, Rucareanu C, Sepulveda FV (1993) Volume-activated chloride channels in HeLa cells are blocked by verapamil and dideoxyforskolin. Pflugers Arch 422:347–353

Epand RM (1778) Proteins and cholesterol-rich domains. Biochim Biophys Acta 1576–1582:2008

Franco R, Torres-Marquez ME, Pasantes-Morales H (2001) Evidence for two mechanisms of amino acid osmolyte release from hippocampal slices. Pflugers Arch 442:791–800

Friis MB, Vorum KG, Lambert IH (2008) Volume-sensitive NADPH oxidase activity and taurine efflux in NIH3T3 mouse fibroblasts. Am J Physiol Cell Physiol 294:C1552–C1565

Gimpl G, Burger K, Politowska E, Ciarkowski J, Fahrenholz F (2000) Oxytocin receptors and cholesterol: interaction and regulation. Exp Physiol 85(spec no.): 41S–49S

Hall JA, Kirk J, Potts JR, Rae C, Kirk K (1996) Anion channel blockers inhibit swelling-activated anion, cation, and nonelectrolyte transport in HeLa cells. Am J Physiol 271:C579–C588

Han X, Budreau AM, Chesney RW (1999) Ser-322 is a critical site for PKC regulation of the MDCK cell taurine transporter (pNCT). J Am Soc Nephrol 10:1874–1879

Haynes MP, Phillips MC, Rothblat GH (2000) Efflux of cholesterol from different cellular pools. Biochemistry 39:4508–4517

Hoffmann EK, Lambert IH (1983) Amino acid transport and cell volume regulation in Ehrlich ascites tumour cells. J Physiol 338:613–625

Hoffmann EK, Lambert IH, Simonsen LO (1986) Separate, Ca^{2+}-activated K^+ and Cl^- transport pathways in Ehrlich ascites tumor cells. J Membr Biol 91:227–244

Hoffmann EK, Lambert IH, Pedersen SF (2009) Physiology of cell volume regulation in vertebrates. Physiol Rev 89:193–277

Holopainen I, Oja SS, Marnela KM, Kontro P (1986) Free amino acids of rat astrocytes in primary culture: changes during cell maturation. Int J Dev Neurosci 4:493–496

Huxtable RJ (1992) Physiological actions of taurine. Physiol Rev 72:101–163

Jacobsen JH, Clement CA, Friis MB, Lambert IH (2008) Casein kinase 2 regulates the active uptake of the organic osmolyte taurine in NIH3T3 mouse fibroblasts. Pflugers Arch 457:327–337

Kabouridis PS, Janzen J, Magee AL, Ley SC (2000) Cholesterol depletion disrupts lipid rafts and modulates the activity of multiple signaling pathways in T lymphocytes. Eur J Immunol 30:954–963

Klausen TK, Hougaard C, Hoffmann EK, Pedersen SF (2006) Cholesterol modulates the volume-regulated anion current in Ehrlich-Lettre ascites cells via effects on Rho and F-actin. Am J Physiol Cell Physiol 291:C757–C771

Kramer JH, Chovan JP, Schaffer SW (1981) Effect of taurine on calcium paradox and ischemic heart-failure. Am J Physiol 240:H238–H246

Lambert IH (1984) Na-dependent taurine uptake in Ehrlich ascites tumor cells. Mol Physiol 6:233–246

Lambert IH (1998) Regulation of the taurine content in Ehrlich ascites tumour cells. Adv Exp Med Biol 442:269–276

Lambert IH (2003a) Reactive oxygen species regulate swelling-induced taurine efflux in NIH3T3 mouse fibroblasts. J Membr Biol 192:19–32

Lambert IH (2003b) Regulation of the volume-sensitive taurine efflux pathway in NIH3T3 mouse fibroblasts. In: Lombardini JB, Schaffer SW, Azuma, J (eds) Taurine in the 21st century, Kluwer Academic/Plenum Publishers, New York, pp 115–122

Lambert IH (2004) Regulation of the cellular content of the organic osmolyte taurine in mammalian cells. Neurochem Res 29:27–63

Lambert IH (2005) Modulation of volume-sensitive taurine release from NIH3T3 mouse fibroblasts by reactive oxygen species. In: Lauf PK, Adragna NC (eds) Cell volume and signalling. Springer, New York, pp 369–378

Lambert IH (2007) Activation and inactivation of the volume-sensitive taurine leak pathway in NIH3T3 fibroblasts and Ehrlich Lettre ascites cells. Am J Physiol Cell Physiol 293:C390–C400

Lambert IH, Falktoft B (2000) Lysophosphatidylcholine induces taurine release from HeLa cells. J Membr Biol 176:175–185

Lambert IH, Falktoft B (2001) Lysophosphatidylcholine-induced taurine release in HeLa cells involves protein kinase activity. Comp Biochem Physiol A Mol Integr Physiol 130:577–584

Lambert IH, Hoffmann EK (1993) Regulation of taurine transport in Ehrlich ascites tumor cells. J Membr Biol 131:67–79

Lambert IH, Hoffmann EK (1994) Cell swelling activates separate taurine and chloride channels in Ehrlich mouse ascites tumor cells. J Membr Biol 142:289–298

Lambert IH, Hoffmann EK, Jorgensen F (1989) Membrane potential, anion and cation conductances in Ehrlich ascites tumor cells. J Membr Biol 111:113–131

Lambert IH, Nielsen JH, Andersen HJ, Ortenblad N (2001) Cellular model for induction of drip loss in meat. J Agric Food Chem 49:4876–4883

Lambert IH, Hoffmann EK, Pedersen SF (2008) Cell volume regulation: physiology and pathophysiology. Acta Physiol Scand 194:255–282

Lambert IH, Klausen TK, Bergdahl A, Hougaard C, Hoffmann EK (2009) Reactive oxygen species activate KCl co-transport in

non-adherent Ehrlich ascites cells but K^+ and Cl^- channels in adherent Ehrlich Lettre and NIH3T3 cells. Am J Physiol Cell Physiol 297:C198–C206

Lang PA, Warskulat U, Heller-Stilb B, Huang DY, Grenz A, Myssina S, Duszenko M, Lang F, Haussingr D, Vallon V, Wieder T (2003) Blunted apoptosis of erythrocytes from taurine transporter deficient mice. Cell Physiol Biochem 13:337–346

Lange Y, Steck TL (2008) Cholesterol homeostasis and the escape tendency (activity) of plasma membrane cholesterol. Prog Lipid Res 47:319–332

Levitan I, Christian AE, Tulenko TN, Rothblat GH (2000) Membrane cholesterol content modulates activation of volume-regulated anion current in bovine endothelial cells. J Gen Physiol 115:405–416

Lim CH, Schoonderwoerd K, Kleijer WJ, de Jonge HR, Tilly BC (2006) Regulation of the cell swelling-activated chloride conductance by cholesterol-rich membrane domains. Acta Physiol (Oxf) 187:295–303

Liu X, Mitrovic AD, Vandenberg RJ (2009) Glycine transporter 1 associates with cholesterol-rich membrane raft microdomains. Biochem Biophys Res Commun 384:530–534

Lowry OH, Rosebrough NJ, Farr AL, Randall RJ (1951) Protein measurement with the Folin phenol reagent. J Biol Chem 193:265–275

Maingret F, Patel AJ, Lesage F, Lazdunski M, Honore E (2000) Lysophospholipids open the two-pore domain mechano-gated K(+) channels TREK-1 and TRAAK. J Biol Chem 275:10128–10133

Mathai JC, Tristram-Nagle S, Nagle JF, Zeidel ML (2008) Structural determinants of water permeability through the lipid membrane. J Gen Physiol 131:69–76

McIntosh TJ, Simon SA (2006) Roles of bilayer material properties in function and distribution of membrane proteins. Annu Rev Biophys Biomol Struct 35:177–198

Mollerup J, Lambert IH (1996) Phosphorylation is involved in the regulation of the taurine influx via the beta-system in Ehrlich ascites tumor cells. J Membr Biol 150:73–82

Mollerup J, Lambert IH (1998) Calyculin A modulates the kinetic constants for the Na^+-coupled taurine transport in Ehrlich ascites tumour cells. Biochim Biophys Acta 1371:335–344

Mongin AA, Reddi JM, Charniga C, Kimelberg HK (1999) [3H]taurine and D-[3H]aspartate release from astrocyte cultures are differently regulated by tyrosine kinases. Am J Physiol 276:C1226–C1230

Moran J, Miranda D, Pena-Segura C, Pasantes-Morales H (1997) Volume regulation in NIH/3T3 cells not expressing P-glycoprotein. II. Chloride and amino acid fluxes. Am J Physiol 272:C1804–C1809

Niu SL, Litman BJ (2002) Determination of membrane cholesterol partition coefficient using a lipid vesicle-cyclodextrin binary system: effect of phospholipid acyl chain unsaturation and headgroup composition. Biophys J 83:3408–3415

Ohtani Y, Irie T, Uekama K, Fukunaga K, Pitha J (1989) Differential effects of alpha-, beta- and gamma-cyclodextrins on human erythrocytes. Eur J Biochem 186:17–22

Ørtenblad N, Young JF, Oksbjerg N, Nielsen JH, Lambert IH (2003) Reactive oxygen species are important mediators of taurine release from skeletal muscle cells. Am J Physiol 284:C1362–C1373

Pasantes-Morales H, Quesada O, Moran J (1998) Taurine: an osmolyte in mammalian tissues. Adv Exp Med Biol 442:209–217

Pedersen S, Lambert IH, Thoroed SM, Hoffmann EK (2000) Hypotonic cell swelling induces translocation of the alpha isoform of cytosolic phospholipase A_2 but not the gamma isoform in Ehrlich ascites tumor cells. Eur J Biochem 267:5531–5539

Pedersen SF, Poulsen KA, Lambert IH (2006) Roles of phospholipase A(2) isoforms in swelling- and melittin-induced arachidonic acid release and taurine efflux in NIH3T3 fibroblasts. Am J Physiol Cell Physiol 291:C1286–C1296

Poulsen KA, Litman T, Eriksen J, Mollerup J, Lambert IH (2002) Downregulation of taurine uptake in multidrug resistant Ehrlich ascites tumor cells. Amino Acids 22:333–350

Poulsen KA, Andersen EC, Hansen CF, Klausen TK, Hougaard C, Lambert IH, Hoffmann EK (2010) Deregulation of apoptotic volume decrease and ionic movements in multidrug-resistant tumor cells: role of chloride channels. Am J Physiol Cell Physiol 298:C14–C25

Pucadyil TJ, Chattopadhyay A (2006) Effect of cholesterol on lateral diffusion of fluorescent lipid probes in native hippocampal membranes. Chem Phys Lipids 143:11–21

Raucci FJ Jr, Wijesinghe DS, Chalfant CE, Baumgarten CM (2010) Exogenous and endogenous ceramides elicit volume-sensitive chloride current in ventricular myocytes. Cardiovasc Res 86(1):55–62

Romanenko VG, Rothblat GH, Levitan I (2004) Sensitivity of volume-regulated anion current to cholesterol structural analogues. J Gen Physiol 123:77–87

Saransaari P, Oja SS (1998) Mechanisms of ischemia-induced taurine release in mouse hippocampal slices. Brain Res 807:118–124

Schuller-Levis GB, Park E (2003) Taurine: new implications for an old amino acid. FEMS Microbiol Lett 226:195–202

Stottrup BL, Keller SL (2006) Phase behavior of lipid monolayers containing DPPC and cholesterol analogs. Biophys J 90:3176–3183

Strancar J, Sentjurc M, Schara M (2000) Fast and accurate characterization of biological membranes by EPR spectral simulations of nitroxides. J Magn Reson 142:254–265

Stutzin A, Torres R, Oporto M, Pacheco P, Eguiguren AL, Cid LP, Sepulveda FV (1999) Separate taurine and chloride efflux pathways activated during regulatory volume decrease. Am J Physiol 277:C392–C402

Swamy MJ, Ciani L, Ge M, Smith AK, Holowka D, Baird B, Freed JH (2006) Coexisting domains in the plasma membranes of live cells characterized by spin-label ESR spectroscopy. Biophys J 90:4452–4465

Uchida S, Kwon HM, Yamauchi A, Preston AS, Marumo F, Handler JS (1992) Molecular cloning of the cDNA for an MDCK cell Na(+)- and Cl(−)-dependent taurine transporter that is regulated by hypertonicity. Proc Natl Acad Sci USA 89:8230–8234

Ullrich N, Caplanusi A, Brone B, Hermans D, Lariviere E, Nilius B, Van Driessche DW, Eggermont J (2006) Stimulation by caveolin-1 of the hypotonicity-induced release of taurine and ATP at basolateral, but not apical, membrane of Caco-2 cells. Am J Physiol Cell Physiol 290:C1287–C1296

Varela D, Simon F, Riveros A, Jorgensen F, Stutzin A (2004) NAD(P)H oxidase-derived H_2O_2 signals chloride channel activation in cell volume regulation and cell proliferation. J Biol Chem 279:13301–13304

Voss JW, Pedersen SF, Christensen ST, Lambert IH (2004) Regulation of the expression and subcellular localisation of the taurine transporter TauT in mouse NIH3T3 fibroblasts. Eur J Biochem 271:4646–4658

Xu X, London E (2000) The effect of sterol structure on membrane lipid domains reveals how cholesterol can induce lipid domain formation. Biochemistry 39:843–849

Yancey PG, Rodrigueza WV, Kilsdonk EP, Stoudt GW, Johnson WJ, Phillips MC, Rothblat GH (1996) Cellular cholesterol efflux mediated by cyclodextrins. Demonstration Of kinetic pools and mechanism of efflux. J Biol Chem 271:16026–16034

Zidovetzki R, Levitan I (2007) Use of cyclodextrins to manipulate plasma membrane cholesterol content: evidence, misconceptions and control strategies. Biochim Biophys Acta 1768:1311–1324